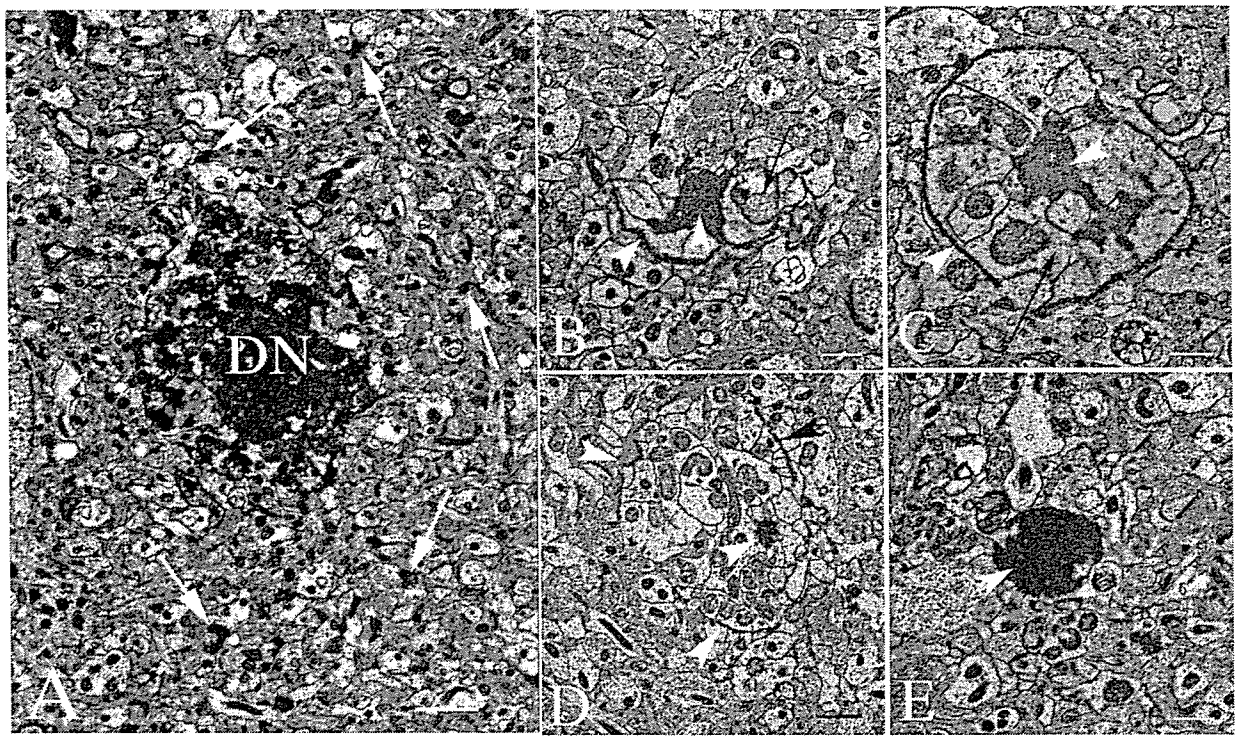

Fig. 3

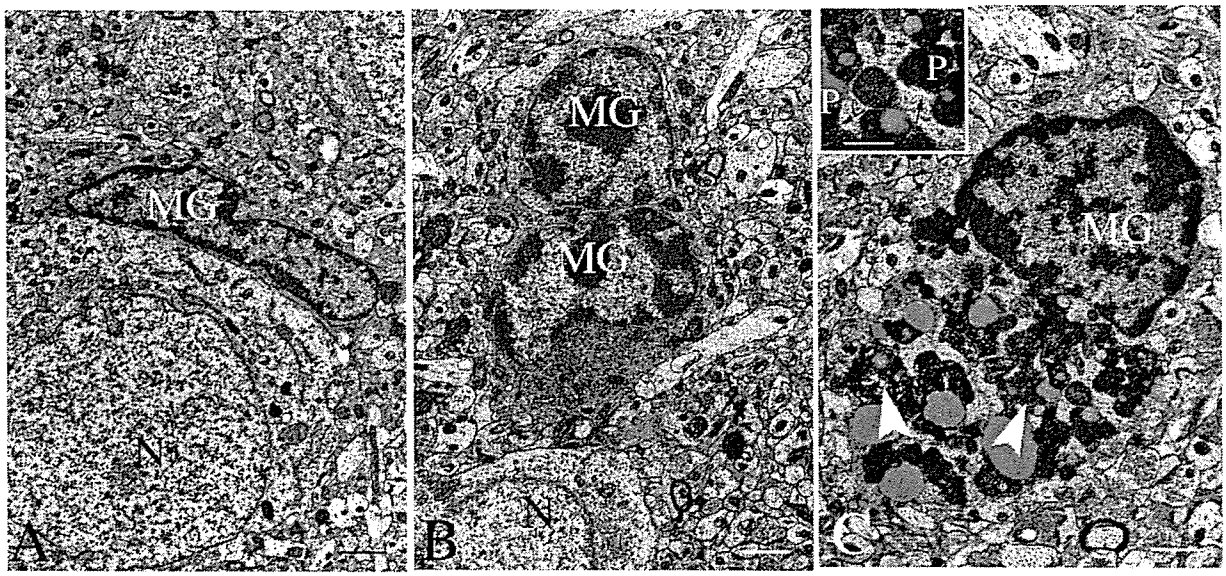

Fig. 4

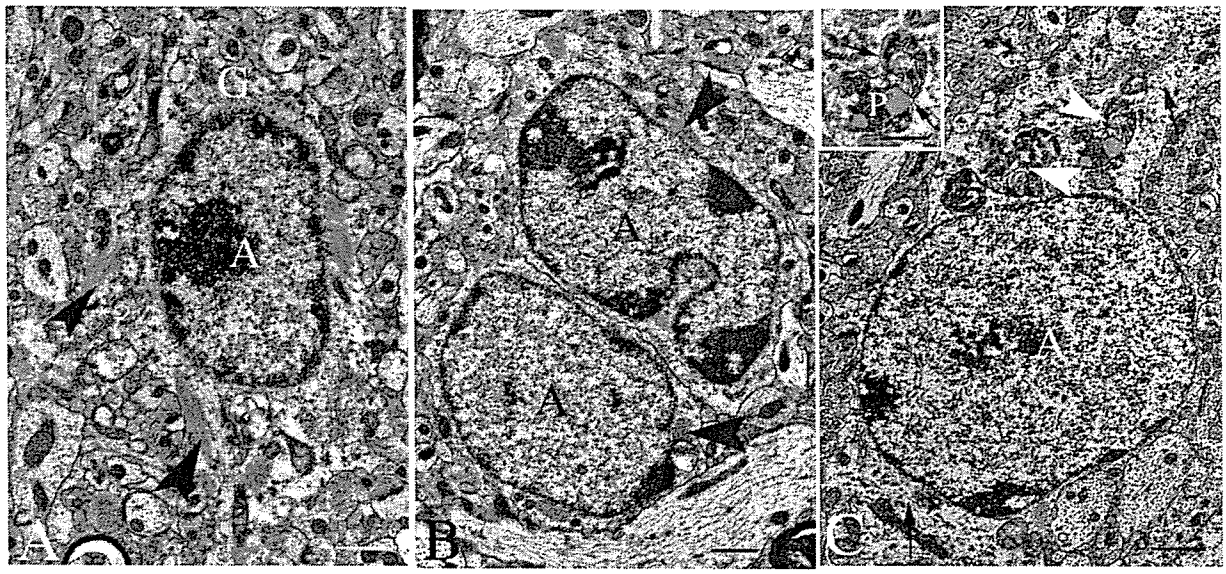

Fig. 5

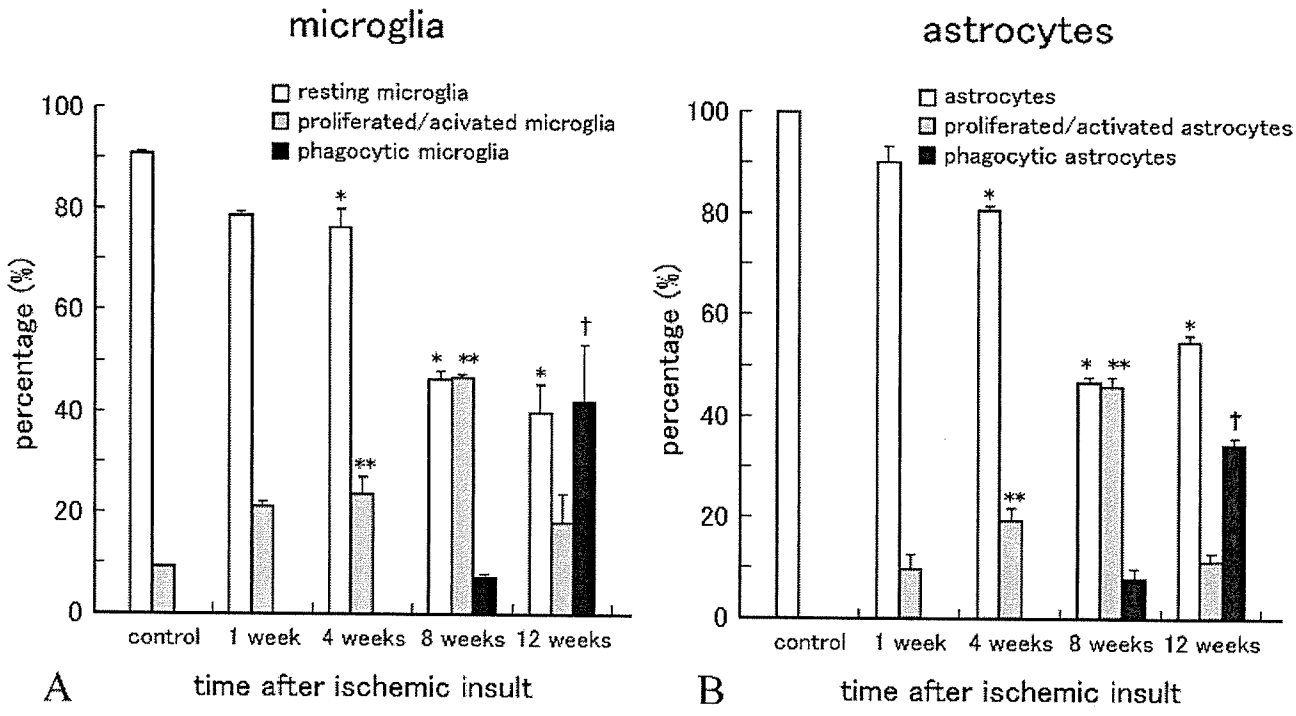

Fig.6

Human Molecular Genetics, 2007, Vol. 16, No. 3 **295–306**
doi:10.1093/hmg/ddl463
Advance Access published on December 21, 2006

Two sites in the *MAPT* region confer genetic risk for Guam ALS/PDC and dementia

Purnima Desai Sundar[1,5], Chang-En Yu[1,5], Weiva Sieh[2], Ellen Steinbart[1,5], Ralph M. Garruto[6], Kiyomitsu Oyanagi[7], Ulla-Katrina Craig[8], Thomas D. Bird[4,5], Ellen M. Wijsman[2,3], Douglas R. Galasko[9] and Gerard D. Schellenberg[1,4,5,*]

[1]Department of Medicine, Division of Gerontology and Geriatric Medicine, [2]Department of Medicine, Division of Medical Genetics, [3]Department of Biostatistics and [4]Department of Neurology and Pharmacology, University of Washington, Seattle, WA 98195, USA, [5]Geriatric Research Education and Clinical Center, Veterans Affairs Puget Sound Health Care System, Seattle Division, Seattle, WA 98108, USA, [6]Department of Anthropology, Laboratory of Biomedical Anthropology and Neurosciences, Binghamton University, SUNY-Binghamton, NY 13902-6000, USA, [7]Department of Neuropathology, Tokyo Metropolitan Institute for Neuroscience, Tokyo, Japan, [8]University of Guam, Mangilao, Guam 96923, USA and [9]Department of Neurosciences, University of California, San Diego, La Jolla CA 92093-0662, USA

Received October 7, 2006; Revised and Accepted December 6, 2006

Unusual forms of amyotrophic lateral sclerosis (ALS-G), Parkinsonism dementia complex (PDC-G) and Guam dementia (GD) are found in Chamorros, the indigenous people of Guam. Neurofibrillary tangles composed of hyperphosphorylated tau are a neuropathologic feature of these closely related disorders. To determine if variation in the gene that encodes microtubule-associated protein tau gene (*MAPT*) contributes to risk for these disorders, we genotyped nine single nucleotide polymorphism (SNP) sites and one insertion/deletion in the 5′ end of *MAPT* in 54 ALS-G, 135 PDC-G, 153 GD and 258 control subjects, all of whom are Chamorros. Variation at three SNPs (sites 2, 6 and 9) influenced risk for ALS-G, PDC-G and GD. SNP2 acts through a dominant mechanism and is independent of the risk conferred by SNPs 6 and 9, the latter two acting by a recessive mechanism. Persons with the high-risk SNP6 and SNP9 AC/AC diplotype had an increased risk of 3-fold [95% confidence interval (CI) = 1.10–8.25] for GD, 4-fold (95% CI = 1.40–11.64) for PDC-G and 6-fold (95% CI = 1.44–32.14) for ALS-G, compared to persons with other diplotypes after adjusting for SNP2. Carriers of the SNP2 G allele had an increased risk of 1.6-fold (95% CI = 1.00–2.62) for GD, 2-fold (95% CI = 1.28–3.66) for PDC-G, and 1.5-fold (95% CI = 0.74–3.00) for ALS-G, compared to non-carriers after adjusting for SNPs 6 and 9. Others have shown that SNP6 is also associated with risk for progressive supranuclear palsy. These two independent *cis*-acting sites presumably influence risk for Guam neurodegenerative disorders by regulating *MAPT* expression.

INTRODUCTION

In the 1950s, amyotrophic lateral sclerosis (ALS) was highly prevalent (143 per 100 000) in Chamorros, the indigenous people of Guam (1). ALS in Guam (ALS-G) is clinically similar to ALS in other populations (1,2). However, unlike typical ALS, where neurodegeneration is confined to spinal cord motor neurons, in ALS-G, central nervous system changes occur including numerous neurofibrillary tangles (NFTs) typically in the neocortex, hippocampus and subcortical regions (2–6). A related disorder, parkinsonism dementia complex (PDC), is also highly prevalent in the same Chamorro population (2,7). The clinical symptoms of PDC in Guam (PDC-G) are parkinsonism (with bradykinesia, gait impairment, rigidity and often resting tremor), accompanied by progressive dementia. The neuropathologic features of PDC-G overlap with ALS-G (4,5,8,9) with a higher NFT burden in brain regions corresponding to the respective clinical

*To whom correspondence should be addressed at: GRECC S-182B, Veterans Affairs Puget Sound Health Care System, 1660 S. Columbian Way, Seattle, WA 98108, USA. Tel: +1 2067642701; Fax: +1 2067642569; Email: zachdad@u.washington.edu.

phenotypes of the two disorders. Spinal cord NFTs are found in both ALS-G and PDC-G (10,11). More recently, late-life dementia without parkinsonism in Chamorros, referred to here as Guam dementia (GD), has been studied (12). The relationships between GD and ALS-G, and PDC-G and Alzheimer's disease (AD) are unclear. Preliminary neuropathology studies suggest that GD has prominent AD-type tangles with less prominent amyloid or neuritic pathology than that found in typical AD (13).

The etiology of ALS-G, PDC-G and GD, collectively referred to here as Guam neurodegenerative disorders, is unknown, though there is substantial evidence supporting a genetic hypothesis. Early work noted highly variable prevalence rates in different Guam villages. Families with multiple cases of ALS-G and PDC-G were common, numerous multigenerational pedigrees with multiple cases of ALS-G, PDC-G or both were described, and the affected father–son pairs were documented (7,14–18). In several studies, 35–40% of probands have relatives with ALS-G/PDC-G (14,17). In the village of Umatac, which had the highest prevalence of the disease (250/100 000) (1), segregation analysis suggested a major gene with penetrance possibly affected by an environmental factor(s) (19). More recently, Plato *et al.* (20), who followed the relatives of a cohort of ALS-G/PDC-G cases and controls for over 40 years, found more new cases in the offspring of affected subjects compared to relatives of controls. Another cluster of ALS and PDC exists on the Kii peninsula of Japan, where the disease is strongly familial (21–25). An environmental hypothesis is also plausible, supported by the decline in incidence of ALS-G over the past 40 years and an increase in onset ages for both ALS-G and PDC-G (2,12,26). No specific environmental factor has been identified though several have been proposed including β-methylamino-alanine (BMAA), a neurotoxin found in cycad seeds (27). The most parsimonious hypothesis is that there are both genetic and environmental components to Guam neurodegenerative disorders.

Identification of the genes that influence susceptibility to Guam neurodegenerative disorders is important to understanding the etiology of these disorders. ALS-G, PDC-G and GD are tauopathies, a class of diseases where aggregated tau (e.g. NFTs) is a prominent neuropathologic feature. For some tauopathies, genetic variation in *MAPT*, the gene that encodes for tau, causes or contributes to the disease. Mutations in *MAPT* cause frontotemporal dementia (FTD) with parkinsonism—chromosome 17 type (FTDP-17) (28–30), an autosomal dominant group of tauopathies with variable phenotypes. However, no *MAPT* mutations have been identified in subjects with Guam disorders (31,32) and the major locus responsible for this disease remains to be found (33). More subtle genetic changes in *MAPT*, presumably in regulatory regions, increase susceptibility to progressive supranuclear palsy (PSP) (34–36), FTD (37–39), corticobasal degeneration (CBD) (40,41) and possibly AD (42), all of which are tauopathies. Although the polymorphic site responsible for elevated risk has been difficult to identify definitively, recent work suggests that alleles at a single nucleotide polymorphism (SNP) in the first intron of tau (intron 0) influence *MAPT* expression and may be the causative site (43). We previously examined 49 ALS-G cases, 82 PDC-G cases and 78 Chamorro controls and reported significant association with the dinucleotide repeat marker CA3662, located 23.9 kb upstream of the transcription start site of *MAPT* (32) (Fig. 1). Since the CA3662 association is likely due to linkage disequilibrium (LD) with the causative variant in the surrounding region, and because recent work on the association between *MAPT* genotypes and PSP implicated SNPs in the 5′ end of *MAPT* (35,43,44), we examined SNPs in corticotrophin-releasing hormone receptor 1 (*CRHR1*) and intramembrane protease 5 (*IMP5*), genes that are upstream of *MAPT*, and SNPs within the 5′ end of *MAPT* (Fig. 1) in a larger case–control dataset of 54 ALS-G, 135 PDC-G, 153 GD and 258 Chamorro controls. We identified two independent regions that contribute to Guam neurodegenerative disorder risk. One is in the *IMP5* region upstream of *MAPT* and acts in a dominant mechanism. The second is in *MAPT*, acts by a recessive mechanism, and possibly corresponds to the same site(s) in *MAPT* that confer risk for PSP.

RESULTS

In the previous work, we showed an allelic association between ALS-G, PDC-G and an allele of a polymorphic site that is 23.9 kb from the 5′ end of *MAPT* (32). Other work showed that for PSP, a tauopathy with some overlapping features with ALS-G and PDC-G, SNP sites within *MAPT* are associated with disease risk (35,43). To determine which polymorphic site(s) in the *MAPT* region contributes to risk of ALS-G and PDC-G, we genotyped eight markers within *MAPT* between the promoter and intron 9, and two in the flanking region 5′ of *MAPT* (Table 1, Fig. 1). Also, we examined the same loci in a GD population to determine if the same alleles confer risk to this related disorder. The cases and controls used were Chamorros ascertained in Guam. Controls were 258 Chamorro subjects with mean age 66.5 ± 14.0 years (35% male) who were cognitively normal, and did not have other neurologic disorders. The case groups were 54 ALS-G subjects (mean age at onset 51.1 ± 11.6 years; 65% male), 135 PDC-G subjects (mean age at onset 64.2 ± 10.1 years; 53% male) and 153 GD cases (mean age at onset 74.9 ± 7.2 years; 27% male).

Allele frequencies for the markers genotyped are given in Table 2. We used marker del-in9 to tag the H1/H2 haplotype system, an inversion polymorphism where approximately 900 kb of chromosome 17 spanning *MAPT* are in opposite orientations in the two haplotypes (45). All SNPs genotyped in this study are within the chromosome 17 segment inverted in this polymorphism. The H1 haplotype is associated with increased risk for PSP and is more common than the H2 haplotype. In our Chamorro samples, the frequency of the H1 haplotype ranged from 95.9% in the PDC-G group to 91.3% in controls (Table 2), which is higher than in typical Caucasian controls (74–80%) (42,45,46). Consistent with previous reports in Caucasians, the H2 haplotype in Chamorros was much less diverse than the H1 haplotype (43,45); nearly all of the SNPs we examined were monomorphic in our sample of H2 haplotypes and we observed strong pairwise LD between the H1/H2 inversion polymorphism and *MAPT* region SNPs in Chamorro subjects. $|D'|$ for the H1/H2

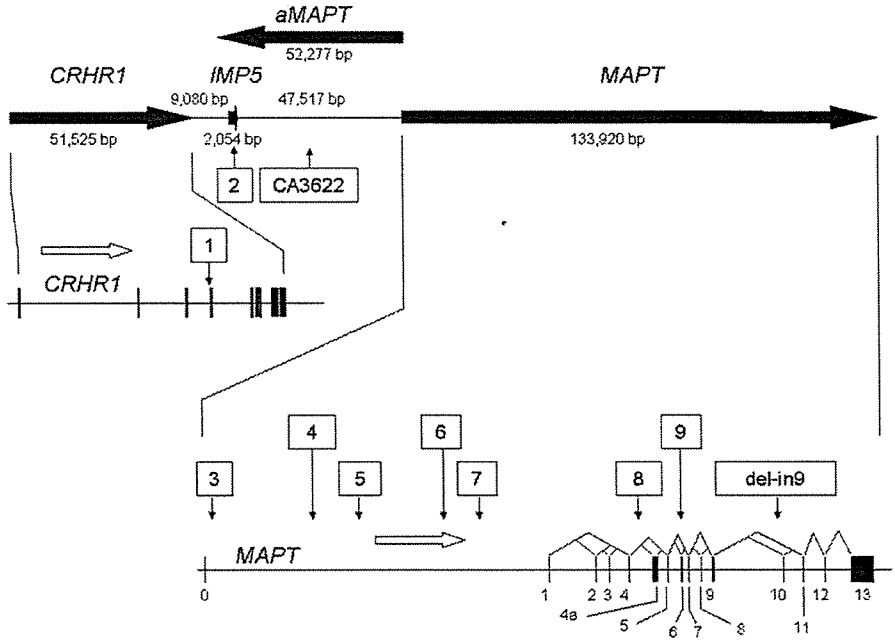

Figure 1. The chromosome 17 *MAPT* region. The distances shown are proportional to the actual sizes of the different genomic elements. Numbers in boxes refer to the SNPs used in this study. The direction of transcription is indicated by the direction of the arrows used to represent *CRHR1*, *IMP5*, *aMAPT* and *MAPT*. Alternatively spliced *MAPT* exons (solid boxes) are indicated by connecting lines above each exon.

inversion polymorphism and nine *MAPT* SNPs, respectively, was 1.0 for SNPs 2 and 3; >0.8 for SNPs 1, 4–6 and 9; and >0.6 for SNPs 6 and 7.

We restricted all subsequent analyses to individuals who are homozygous for the H1 lineage, for two reasons. First, the Chamorro people of Guam have a much higher incidence of ALS than Caucasians and PDC-G does not have a clinicopathological equivalent in Caucasians. Since Chamorros and Caucasians also have a different H1 frequency, a disease association involving SNPs that are associated with the inversion polymorphism could reflect the confounding effect of population admixture rather than a true disease association. Second, since inversions result in suppression of recombination, the H1 and H2 lineages represent evolutionarily and reproductively isolated regions of the genome even within a panmictic population. Therefore, analysis of just one of these lineages is necessary to permit evaluation of individual SNP effects separately from effects attributable to the inversion polymorphism. LD patterns among the nine *MAPT* region SNPs in 214 H1/H1 controls are shown in Table 3. LD was strongest ($|D'| \geq 0.8$ and/or $r^2 \geq 0.4$) between SNPs 1–2, 3–5, 6–7 and 8–9, and was relatively weak between the other SNPs.

Global differences in allele frequencies for SNPs 2 ($P = 0.007$), 6 ($P = 0.011$), 7 ($P = 0.055$) and 9 ($P = 0.032$) were observed among H1 homozygotes in the ALS-G, PDC-G, GD and control groups (Table 2). Allele frequencies did not differ significantly among the three case groups. Compared to controls, cases tended to have higher frequencies of the minor 'A' allele at SNP2, major 'A' allele at SNP6, major 'A' allele at SNP7 and major 'C' allele at SNP9. There was no evidence of Hardy–Weinberg disequilibrium (HWD) at any of the nine SNPs in H1/H1 controls or cases with PDC-G or GD. However, Hardy–Weinberg equilibrium in the 49 H1/H1 ALS-G cases was rejected at SNPs 3 ($P = 0.004$), 4 ($P = 0.010$) and 5 ($P = 0.023$). Whereas allelic association tests are susceptible to false-positive results as a consequence of HWD, genotypic association tests remain valid (47). Global genotypic (Table 4) and allelic (Table 2) association screening tests yielded comparable results for SNPs 2, 6, 7 and 9. Exploratory analyses were also conducted for SNPs 3 and 5 based on the global genotype association test results, and possible univariate associations with ALS-G or PDC-G (data not shown, Supplementary Material, Table S1).

Univariate logistic regression analyses showed that the risk of GD and PDC-G in Guam was significantly associated with SNPs 2, 6, 7 and 9 (Table 4). Evidence for association was also found for SNP3 and ALS-G (data not shown, Supplementary Material, Table S1), although the number of ALS-G cases was relatively small. The G allele of SNP2 in *IMP5* conferred increased risk in a dominant manner, whereas the SNP5–7 A and SNP3 and 9 C alleles appear to confer risk in a recessive manner (Table 4, data not shown, Supplementary Material, Table S1). *MAPT* region SNPs were fit as either dominant or recessive genetic effects in higher order models for the sake of model parsimony. No significant evidence of an association was found between Apolipoprotein E (*APOE*) and ALS-G, PDC-G or GD in Guam (Table 2).

A fortuitous aspect of the data allowed us to infer that the associations observed for SNPs 6 and 7 could largely be explained by SNP6. All 181 H1/H1 individuals with the

Table 1. Polymorphic sites

SNP/ polymorphism	dbSNP number	Gene	Sequence location (bp)	Alleles	Distance to next SNP	Assay type	PCR primers or TaqMan assay number	Restriction enzyme or reporter sequence
1	rs242937	*CRHR1* (intron 3)	41,254,149	A,G	24,811	RFLP	F-GCTCTACCACAAG AAGCCCTGTC R-CTGGGCTGTTCC TTTGCAAGT	MnlI
2	rs242944	*IMP5* (exon 1)	41,278,960	A,G	49,751	TaqMan	C_2257672_10	
3	rs3744457	*MAPT* (intron 0)	41,328,711	C,T	20,493	RFLP	F-CACTTTAGTTGCC CTTCCCCCT R-CTCCGAGCGCTG AGAAAGAAAT	NlaIII
4	rs3785880	*MAPT* (intron 0)	41,349,204	T,G	9,256	TaqMan	F-GGCACTGCTGGT TTGAAAGG R-TGGGCAGGGTG TGAATCC	[VIC] CCACGG**C** AGTTACT [FAM] CCACGG **A**AGTTACT
5	rs2055797	*MAPT* (intron 0)	41,358,460	A,T	17,113	TaqMan	F-CAAACCGTCTTG CACAGTGT R-GGCTGCAGTGG TTTCTTCAG	[VIC] CCCTCTC C**T**GGGTTT [FAM] CCTCTCC **A**GGGTTT
6	rs242557	*MAPT* (intron 0)	41,375,573	A,G	7,226	TaqMan	F-CGTTTCTTCTTCC TTACAAAGCAGTT R-CCCTGGTCCCGT GACA	[VIC] CCCAGGG T**A**CACCAG [FAM] CCAGGGT **G**CACCAG
7	rs242562	*MAPT* (intron 0)	41,382,599	A,G	32,166	TaqMan	C_3202957_10	
8	rs2435207	*MAPT* (intron 4)	41,414,765	A,G	8,454	TaqMan	F-CGTGCAGAGCCC TTCCT R-AGAAGCCCCATTC AGATCTATCCA	[VIC] CTTGTCTG TG**A**TCAGTG [FAM] CTTGTCT GTG**G**TCAGTG
9	rs2258689	*MAPT* (exon 6)	41,423,219	C,T	18	TaqMan	F-GTGCCCAGAGCC ACCTT R-CTGCCAGTTCGG GAAGTGA	[VIC] CAGAAGA GACGT**G**TTTAG [FAM]CAGAAGA GACGT**A**TTTAG
del-in9		*MAPT* (intron 9)	41,442,488	H1,H2	19,297	fragment size	F-GGAAGACGTTCTCACT GATCTG R-AGGAGTCTGGCTTCAG TCTCTC	

The sequence location is from NCBI Build 36.1. Nucleotides in boldface are alleles of SNPs.

Table 2. Allele frequencies by C17 inversion status and diagnosis group

SNP	Alleles (major/minor)	All H1 and H2 genotypes				H1/H1 homozygotes only				
		Controls ($n = 258$)[a]	GD ($n = 153$)	PDC-G ($n = 135$)	ALS-G ($n = 54$)	Controls ($n = 214$)	GD ($n = 136$)	PDC-G ($n = 124$)	ALS-G ($n = 49$)	P^*
Markers 5′ to *MAPT*										
1[b]	G/A	24.7	24.5	26.5	17.6	17.7	19.6	23.2	13.3	0.149
2[c]	A/G	40.6	46.1	50.4	42.6	34.4	42.3	47.6	40.8	0.007
MAPT markers										
3[d]	C/T	50.0	47.1	40.7	44.4	44.9	44.5	39.0	40.8	0.453
4[e]	T/G	33.3	34.3	28.7	33.3	36.3	37.1	30.9	34.7	0.445
5	A/T	48.6	42.2	37.8	44.4	43.9	39.0	35.9	40.8	0.210
6	A/G	51.4	40.5	39.3	45.4	47.4	36.8	36.7	40.8	0.011
7[f]	A/G	44.9	36.3	34.4	40.7	40.6	32.4	31.4	36.7	0.055
8	G/A	16.1	12.1	13.7	16.7	17.1	12.9	14.9	17.4	0.458
9[g]	C/T	50.2	39.2	39.9	41.7	45.5	35.3	37.3	37.8	0.032
del-in9	H1/H2	8.7	5.9	4.1	4.6					
APOE	ε2	4.5	4.0	6.7	1.9	4.9	4.2	6.1	2.0	0.523
	ε3	90.5	91.2	90.3	90.7	90.2	91.7	90.7	90.8	
	ε4	5.0	4.7	3.0	7.4	4.9	4.2	3.2	7.1	

Minor allele frequency for diallelic variants; all allele frequencies for *APOE*, a triallelic variant system.
*Fisher's exact test of global allele frequency differences among H1 homozygotes in the four diagnosis groups.
[a]*n*, total number of individuals; 2*n*, total number of alleles.
[b]Two H1/H1 controls, one H2/H2 control, six H1/H1 GD cases and one H1/H1 PDC case had missing genotypes at this site.
[c]Two H1/H1 controls had missing genotypes at this site.
[d]One H1/H1 PDC case had a missing genotype at this site.
[e]Three H1/H1 controls, one H1/H2 control and one H1/H1 PDC case had missing genotypes at this site.
[f]Two H1/H1 controls had missing genotypes at this site.
[g]One H1/H1 control and two H1/H1 PDC cases had missing genotypes at this site.

high-risk A/A genotype at SNP6 also had the high-risk A/A genotype at SNP7 with the exception of two PDC-G cases, who had the low-risk G/A genotype at SNP7. The SNP6 A allele was therefore a nearly perfect marker for the AA haplotype at SNPs 6 and 7 in this population. In contrast, 39/218 (17.9%) H1/H1 individuals with the high-risk A/A genotype at SNP7 had the low-risk G/A or G/G genotypes at SNP6. If the homozygous AA diplotype at SNPs 6 and 7 were truly responsible for disease, then using the SNP7 rather than SNP6 A/A genotype as a marker would lead to an attenuated estimate of the genetic effect because of the noise introduced by including 39 individuals with the low-risk GA/AA or GA/GA diplotypes at SNPs 6 and 7 into the 'exposed' category. Furthermore, including both SNPs 6 and 7 in the model would reduce the statistical significance of either effect because they are measures of the same underlying haplotype. The magnitude of the estimated risks of GD, PDC-G or ALS-G associated with SNP6 were stronger than SNP7 in both univariate (Table 4) and higher order models, and neither SNP was statistically significant when both were included in the model. These results indicated that the homozygous AA diplotype at SNPs 6 and 7, almost perfectly captured by the SNP6 A/A genotype, was associated with disease risk.

Combinations of two or more *MAPT* SNPs were analyzed to identify independent risk factors and interactions between genetic variants. Possession of the 'G' allele at SNP2 was an independent risk factor for both GD and PDC-G as well as for all cases combined (Table 5). Additionally, a significant interaction between the high-risk A/A and C/C genotypes at SNPs 6 and 9 was found for all three case groups and the combined set of cases. No significant three-way interaction was found, and *APOE* did not confound or weaken the *MAPT* effects.

The final genetic model for GD and PDC-G included SNP2 and the main effects and interaction of SNPs 6 and 9 (Table 5). When the final genetic model for GD and PDC-G was fit for ALS-G, a similar risk pattern emerged (Table 5). H1/H1 persons with the homozygous AC diplotype at SNPs 6 and 9 had a 3-fold [95% confidence interval (CI) = 1.10–8.25] increased risk of GD, 4-fold (95% CI = 1.40–11.64) increased risk of PDC-G and 6-fold (95% CI = 1.44–32.14) increased risk of ALS-G, compared to persons who were not homozygous for this diplotype after adjusting for SNP2. H1/H1 carriers of the SNP2 G allele had a 1.6-fold (95% CI = 1.00–2.62) increased risk of GD, 2-fold (95% CI = 1.28–3.66) increased risk of PDC-G and 1.5-fold (95% CI = 0.74–3.00) increased risk of ALS compared to non-carriers after adjusting for SNPs 6 and 9. In an analysis of all cases combined, the risk of developing GD, PDC-G or ALS-G was independently increased by 1.7-fold (95% CI = 1.18–2.60) in carriers of the SNP2 G allele, and 3.8-fold (95% CI = 1.64–8.78) in persons with the homozygous AC diplotype at SNPs 6 and 9.

The high-risk AC diplotype, or haplotype, defined by SNPs 6 and 9 is unlikely to represent the H1c haplotype reported to be associated with PSP and CBD (36). The frequency of H1 haplotypes containing this AC haplotype was significantly higher in the case samples (0.484–0.525) than in the control samples (0.355), as was the 3-SNP haplotype, TAC, that also includes SNP4 (frequency 0.415–0.437 in the case samples versus 0.296 in the control samples) (Supplementary Material, Table S3). Although the A allele of SNP6 is the

Table 3. Pairwise LD among SNPs in Guam H1/H1 controls

		r^2-value								
		1[a]	2	3	4	5	6	7	8	9
$\|D'\|$	1[a]	–	0.40	0.00	0.00	0.00	0.03	0.02	0.01	0.08
	2	1.00	–	0.09	0.04	0.12	0.17	0.11	0.00	0.00
	3	0.08	0.47	–	0.66	0.70	0.21	0.13	0.03	0.02
	4	0.08	0.35	0.98	–	0.47	0.10	0.22	0.05	0.00
	5	0.07	0.53	0.85	0.80	–	0.34	0.22	0.02	0.02
	6	0.38	0.61	0.48	0.40	0.62	–	0.58	0.01	0.04
	7	0.34	0.56	0.39	0.52	0.50	0.87	–	0.02	0.01
	8	0.09	0.14	0.36	0.36	0.24	0.15	0.25	–	0.25
	9	0.54	0.04	0.14	0.04	0.13	0.22	0.09	1.00	–

[a]Numbers in the left most column and the top row refer to the polymorphism site numbers in Table 1.

allele on the H1c haplotype, estimation of 5-SNP haplotypes (including the three SNPs used to tag H1c) in the JPT HapMap sample shows that the frequency of the H1c haplotype is only 2.4% (Supplementary Material, Table S4). Also, the C allele of SNP9 perfectly predicts the existence of allele C for SNP rs2471738. Since the H1c haplotype has allele T for rs2471738, based on the JPT 5-SNP haplotype frequencies, the conditional probability that the SNP6–9 AC haplotype (or the SNP4–6–9 TAC haplotype) represents that the H1c haplotype is 0.

DISCUSSION

The results described above show that genetic variation in the *MAPT* region contributes to risk for ALS-G, PDC-G and GD. Our previous work (32) showed an association between a single polymorphism (CA3662, Fig. 1) and ALS-G and PDC-G. Here, we confirm and extend our original findings by showing risk associated with additional SNPs in a larger sample. Also, these results extend our findings to GD, which was not previously studied. An intriguing novel finding is that the risk for Guam neurologic disorders is independently determined by SNPs in two different locations, one within *MAPT* and another upstream of *MAPT* in or near *IMP5*.

Genotypes within *MAPT* contribute to susceptibility to Guam neurologic disorders by a recessive mechanism. For SNPs 6, 7 and 9, homozygous genotypes (A/A, A/A and C/C, respectively) confer risk, whereas the other 2 genotypes for each site do not (Table 4). In studies of PSP, SNP6 genotypes also show a statistically significant association with risk (43,44), and in both our study and the work on PSP, the A allele is the high-risk allele. SNP6, located in the first intron of *MAPT* (Fig. 1), is in a region conserved across a number of mammalian species (43,48) suggesting a functional role in *MAPT* regulation. Rademaker *et al.* (43) showed that the 182 bp region containing SNP6 can act as a *cis*-acting transcriptional enhancer in a cell culture model and that the enhancer activity was greater when the SNP6 G allele was present compared to the A allele. Thus, for both Guam neurologic disorders and PSP, SNP6 may be the site, or at least one of the sites that determines disease risk, as opposed to some other close marker in LD with SNP6. This hypothesis is strengthened by the observation that even though the high-risk SNP6 allele is the same in the Chamarro as in other populations, the high-risk haplotype in the Chamarro population does not appear to be the H1c haplotype, previously reported to be associated with other neurological diseases (36). In fact, despite the higher frequency of ALS/PDC, the H1c haplotype appears to be much rarer in this population than in populations of European descent, which is inconsistent with a major role of H1c as a contributor to risk of ALS/PDC.

In our study, genotypes at SNP9 interact with SNP6 genotypes to increase risk. SNP9 is a non-synonymous change in exon 6, which is a coding exon. This exon is alternatively spliced and is present in approximately 20–40% of transcripts in the hippocampus and cerebellum, and approximately 10% of transcripts in the cortex (49). However, exon 6 sequences are not present in the aggregated pathologic tau. Thus, it is not clear at this point whether SNP9 functions in a regulatory fashion, or if it simply marks some other polymorphic site that is the true functional polymorphism. The regulation of *MAPT* expression is certainly complex. In addition to the enhancer sequence noted above, mutations that affect the regulation of alternative splicing have a profound effect on disease risk (29,30,50). Thus SNPs 6 and 9 may be in two different regulatory regions of *MAPT*. The fact that the genotypes interact suggests a *cis*-acting mechanism.

A novel finding of our work is that there is a second region marked by SNP2 that is 5′ to *MAPT* and that acts independently of sites within *MAPT* to confer risk. Unlike SNPs 6 and 9, for SNP2, the G allele acts by a dominant mechanism. There are several possible hypotheses as to how SNP2 could influence risk for Guam disease. Perhaps, the most likely hypothesis is that SNP2 or an SNP in LD with SNP2 is in a *cis*-acting regulatory sequence that influences *MAPT* expression. Another related hypothesis is that SNP2 is in LD with polymorphic site in this region that influences the expression of another gene, provisionally called antisense to *MAPT* (*aMAPT*). This gene is transcribed in the opposite direction as *MAPT* and *IMP5*, has a transcription start site in *MAPT* intron 0, and extends past *IMP5* (Fig. 1). *aMAPT* has multiple alternatively spliced forms with one exon overlapping with exon 0 of *MAPT*. This gene may act as a natural antisense regulatory sequence that controls *MAPT* expression (Ian D'Souza, personal communication). It is not clear at present whether the *aMAPT* sequence is translated into a protein. Thus, polymorphic sites 5′ to *MAPT* could influence

Table 4. Univariate logistic regression models of the risk of GD, PDC-G, or ALS-G associated with variants among chromosome 17 H1 homozygotes on Guam

SNP	Genotype	Controls *n*(%)	GD *n*(%)	OR (95% CI)	$P^* > \chi^2_{2df}$	PDC-G *n*(%)	OR (95% CI)	$P^* > \chi^2_{2df}$	ALS-G *n*(%)	OR (95% CI)	$P^* > \chi^2_{2df}$	Global P^{**}
2	A/A	94 (44.3)	42 (30.9)	Referent	0.040	30 (24.2)	Referent	0.001	16 (32.6)	Referent	0.306	0.013
	G/A	90 (42.5)	73 (53.7)	1.82 (1.13–2.93)***		70 (56.5)	2.44 (1.45–4.08)***		26 (53.1)	1.70 (0.85–3.37)		
	G/G	28 (13.2)	21 (15.4)	1.68 (0.86–3.29)		24 (19.4)	2.69 (1.36–5.32)***		7 (14.3)	1.47 (0.55–3.93)		
	A/A	94 (44.3)	42 (30.9)	Referent		30 (24.2)	Referent		16 (32.6)	Referent		
	G/–	118 (55.7)	94 (69.1)	1.78 (1.13–2.81)***		94 (75.8)	2.50 (1.53–4.08)***		33 (67.3)	1.64 (0.85–3.17)		
6	A/A	53 (24.8)	56 (41.2)	Referent	0.006	53 (42.7)	Referent	0.003	19 (38.8)	Referent	0.112	0.009
	A/G	119 (55.6)	60 (44.1)	0.48 (0.29–0.78)***		51 (41.1)	0.43 (0.26–0.71)***		20 (40.8)	0.47 (0.23–0.95)***		
	G/G	42 (19.6)	20 (14.7)	0.45 (0.23–0.86)***		20 (16.1)	0.48 (0.25–0.92)***		10 (20.4)	0.66 (0.28–1.58)		
	G/–	161 (75.2)	80 (58.8)	Referent		71 (57.3)	Referent		30 (61.2)	Referent		
	A/A	53 (24.8)	56 (41.2)	2.13 (1.34–3.37)***		53 (42.7)	2.27 (1.41–3.64)***		19 (38.8)	1.92 (1.00–3.70)***		
7	A/A	70 (33.0)	66 (48.5)	Referent	0.012	61 (49.2)	Referent	0.013	21 (42.9)	Referent	0.306	0.038
	G/A	112 (52.8)	52 (38.2)	0.49 (0.31–0.79)***		48 (38.7)	0.49 (0.30–0.80)***		20 (40.8)	0.60 (0.30–1.18)		
	G/G	30 (14.2)	18 (13.2)	0.64 (0.32–1.25)		15 (12.1)	0.57 (0.28–1.17)		8 (16.3)	0.89 (0.35–2.23)		
	G/–	142 (67.0)	70 (51.5)	Referent		63 (50.8)	Referent		28 (57.1)	Referent		
	A/A	70 (33.0)	66 (48.5)	1.91 (1.23–2.97)***		61 (49.2)	1.96 (1.25–3.09)***		21 (42.9)	1.52 (0.81–2.87)		
9	C/C	61 (28.6)	59 (43.4)	Referent	0.017	52 (42.6)	Referent	0.033	19 (38.8)	Referent	0.348	0.079
	T/C	110 (51.6)	58 (42.6)	0.55 (0.34–0.88)***		49 (40.2)	0.52 (0.32–0.86)***		23 (46.9)	0.67 (0.34–1.33)		
	T/T	42 (19.7)	19 (14.0)	0.47 (0.24–0.90)***		21 (17.2)	0.59 (0.31–1.11)		7 (14.3)	0.54 (0.21–1.39)		
	T/–	152 (71.4)	77 (56.6)	Referent		70 (57.4)	Referent		30 (61.2)	Referent		
	C/C	61 (28.6)	59 (43.4)	1.91 (1.22–3.00)***		52 (42.6)	1.85 (1.16–2.95)***		19 (38.8)	1.58 (0.83–3.01)		

*Model χ^2 for logistic regression of disease status on the three genotype categories for each SNP.
**Fisher's exact test of global genotype frequency differences among chromosome 17 H1 homozygotes in the four diagnosis groups.
***P-value$\leq$0.05 for the effect of the given genotype compared to the referent group estimated using logistic regression.

Table 5. Risk of GD, PDC-G or ALS-G associated with *MAPT* region variants on Guam

MAPT SNP effects	GD OR (95% CI)	PDC-G OR (95% CI)	ALS-G OR (95% CI)	GD, PDC-G or ALS-G OR (95% CI)
2	1.61 (1.00–2.62)	2.16 (1.28–3.66)	1.49 (0.74–3.00)	1.76 (1.18-2.60)
6	0.97 (0.49–1.93)	0.85 (0.42–1.73)	0.66 (0.23–1.93)	0.87 (0.50–1.52)
9	1.06 (0.57–1.97)	0.83 (0.42–1.63)	0.60 (0.21–1.67)	0.88 (0.53–1.46)
6 and 9	3.02 (1.10–8.25)	4.04 (1.40–11.64)	6.80 (1.44–32.14)	3.79 (1.64–8.78)

Analysis was restricted to H1 homozygotes which were 211 controls, 136 GD, 122 PDC-G and 49 ALS-G cases with non-missing genotypes.

aMAPT expression, which in turn would influence *MAPT* expression. Another hypothesis is that the gene product of *IMP5* is involved in Guam disease pathogenesis. SNP2 is a non-synonymous (H303R) change in the potential coding region of *IMP5*, a gene predicted from a number of unspliced expressed sequences in public databases. The predicted amino acid sequence for *IMP5* has strong homology to signal peptide peptidases and weaker homology to presenilin1 and 2 (*PSEN1* and *PSEN2*) (51). Because mutations in *PSEN1* and *PSEN2* cause AD, which is a tauopathy, variability at SNP2 could alter the function of *IMP5* and thus influence risk for Guam disease. *PSEN1* and *PSEN2* are components of a transmembrane protease that causes the γ-secretase cleavage of amyloid precursor protein (APP). This cleavage contributes to the production of an APP fragment called Aβ, which is the primary component of the amyloid plaques in AD. Mutations in *PSEN1* or *PSEN2* alter the γ-secretase cleavage site resulting in a more toxic form of Aβ. However, this hypothesis seems unlikely for the following reasons. First, Aβ deposition is not a feature of ALS-G or PDC-G. Second, there is no data available on whether *IMP5* transcripts are translated to produce a protein. Third, *IMP5* is not strongly homologous to the presenilins. Fourth, the active site aspartates in *IMP5* are in opposite orientation to the presenilins making it unlikely that *IMP5* would cleave APP and thus would not be involved in Aβ production (51). Thus, it is more likely that the risk allele of SNP2 or another SNP in LD with SNP2 influences the regulation of *MAPT* and thus influences the disease process.

The SNP alleles described here are not likely to cause ALS-G, PDG-G or GD, but rather increase risk in combination with other genetic and environmental factors. This conclusion is based on the fact that not all affected subjects have the high-risk alleles, and not all carriers of the high-risk allele have the disease. Also, an earlier analysis of a component of a large pedigree from the village of Umatac found evidence against linkage of *MAPT* and ALS-G/PDC-G (32). The drop in prevalence of ALS-G and the increase in onset ages for both ALS-G and PDC-G over the past few decades suggest a change in exposure to an unknown environmental factor(s), and are not consistent with outbreeding diluting a genetic factor(s). Dietary BMAA (27,52) found in cycad seeds is one candidate for an environmental toxin. Our finding that picking, processing and eating cycads elevate risk for Guam disease (Borenstein, Mortimer, Dahlquist, Wu, Salmon, Gamst, Olichney, Thal, Silbert, Kaye, Adonay, Craig, Schellenberg and Galasko, submitted for publication) supports the hypothesis that BMAA may be an environmental susceptibility factor that potentially interacts with *MAPT* region alleles to increase risk for Guam disease. However, attempts to model neurodegeneration in animals by feeding BMAA-containing flour derived from cycad seeds, as prepared by Chamorros in Guam, required unrealistically large doses to produce an effect (53–55). A major environmental change in Guam is the post-World War II improvement in general diet. Perhaps, comparison of the environment in Guam to that of the Kii peninsula of Japan, where a cluster of very similar familial ALS and PDC cases occurs (21–25) will help identify common environmental and genetic factors.

The work presented here is the first genetic study of GD. Our working hypothesis is that GD is a variation of the same disease as ALS-G and PDC-G, and that the symptoms observed are more a function of when onset occurs rather than the underlying genetic and environmental architecture of these disorders. The fact that the same pattern of risk is observed for multiple SNPs for GD, ALS-G and PDC-G argues for a common disease mechanism involving tau. However, the underlying primary genetic architecture and environmental influence for each of these three Guam disorders is not known and could still be distinct for each, even though a common neurodegenerative pathway is the end result. The *APOE* and *MAPT* region results certainly argue that GD and AD are distinct. In all forms of Guam disease, the ε4 and ε2 *APOE* allele frequencies are not significantly different between cases and controls (Table 2). The remarkably low ε4 frequency for controls (5%, Table 2) is consistent with other Asian populations where the ε4 frequency is typically lower than Caucasian frequencies (56). In almost all AD populations, with few exceptions, ε4 frequencies are elevated relative to controls, even when the control frequency is low (56). In most AD studies to date (57–64), with some exceptions (42,65–69), there appears to be no association between polymorphic sites in *MAPT* and AD. Results from the SNP2 region in AD cohorts have not been described. Arguing against the hypothesis that GD is distinct from AD is that these two disorders are not clinically distinguishable. Additional autopsies for GD cases are needed to establish the relationships between GD and ALS-G, and PDC-G and AD.

The observation that the same SNP (SNP6) influences risk for Guam neurologic disorders and PSP (43) and that other tauopathies such as FTD (37) and CBD (40,41) also show an association with *MAPT* region alleles, argues that these disorders at least partially share a common disease mechanism. The common feature of these diseases is aggregated tau occurring as NFTs, and in the case of PSP, also in glial cells. *MAPT* genetic variation may also play a role in typical Parkinson

disease (PD) (46), which is not a tauopathy. The differences between these disorders are intriguing since the localization of neurodegenerative changes and the associated clinical symptoms vary remarkably between ALS-G, PDC-G, GD, PSP, PD and CBD. Presumably, the difference is the result of other unknown environmental and genetic factors, though the difference could also be due to the interactions between genetic variations in the *IMP5* region versus variation within *MAPT*.

METHODS

Subjects

The Chamorro subjects included in this study were recruited through a series of studies in Guam. Archival clinical data and DNA samples were obtained from the National Institutes of Neurological and Communicative Disorders and Stroke Intramural Research program in Guam (1956–83, Ralph Garruto) and from Kiyomitsu Oyanagi. Diagnoses of ALS and PDC were confirmed by examination of case records including autopsy reports, which were available on many patients. More recently, subjects in Guam were evaluated through the University of Guam–University of California, San Diego Consortium (1995–2006) as part of an NIH Program Project Grant. All subjects (or proxies in the case of demented patients who lacked decisional capacity) provided written informed consent to participate in the study, and the study was approved by Institutional Review Boards at the University of Guam, UCSD and University of Washington. Details regarding subject recruitment and medical evaluation were described previously (12). Briefly, all subjects were first evaluated by medical history, physical examination, and cognitive testing using the Cognitive Abilities Screening Instrument (CASI). Subjects who failed the CASI (cutoff score $\leq$75/100) or with a history or screening physical examination suggestive of neurologic disease underwent a further structured neurological examination that included the Unified Parkinson Disease Rating Scale, a standardized psychometric test battery, and blood tests. Neuroimaging with head CT or MRI was obtained when possible. Consensus diagnoses were made by 3 neurologists after reviewing all relevant information and using standard clinical diagnostic criteria wherever possible. The diagnosis of PDC required insidious onset and gradual progression of primary parkinsonism and dementia, either of which could be the initial feature. However, the onset of parkinsonism during mild-to-moderate stage of dementia was necessary to diagnose PDC. Parkinsonism first noted in patients with severe or end-stage dementia was considered a secondary feature of GD. Dementia was diagnosed using the Diagnostic and Statistical Manual, fourth edition (DSM-IV) criteria (American Psychiatric Association, 1994). The pure dementia syndrome in Guam resembled AD clinically, and many patients met the NINCDS/ADRDA criteria for probable AD (70). Patients with this dementia profile who had additional factors such as stroke and depression met criteria for possible AD. Controls were subjects without any neurologic disorder or dementia. Subjects classified as controls had a CASI score $\geq$80, were functionally independent, and lacked motor weakness, tremor or gait difficulty on a brief screening exam. Subjects with a CASI score $<$80 were classified as controls only if detailed neurological and psychometric evaluation showed no evidence of dementia, mild cognitive impairment or any neurological disorder.

Polymorphic loci and genotyping

Genomic DNA was isolated either from available frozen brain tissue or fresh blood samples from case and control subjects. *APOE* genotypes were determined by a modification of the method of Hixson and Vernier (71). Some SNPs in the *MAPT* region were genotyped as restriction-fragment-length polymorphisms (Table 1). For these loci, short DNA fragments containing the polymorphic sites were produced by polymerase chain amplification (PCR), digested with the appropriate restriction enzyme, the resulting fragments resolved using agarose gel electrophoresis, and fragments visualized with ethidium bromide. Locus del-in9 is an insertion/deletion polymorphism. PCR products spanning this locus differ by 238 bp depending on the presence or absence of the insertion. Size differences were observed using agarose gel electrophoresis. The remaining SNPs were genotyped using TaqMan allele discrimination assays (Applied Biosystems, CA, USA) (Table 1). SNPs were selected after initially screening 18 SNPs in a panel of 16 Chamorro controls (Supplementary Material, Table S2). SNPs were selected as follows. The del-in9 polymorphism was selected because it is a tagging site for the H1/H2 haplotype. SNPs 1 and 2 in genes *CRHR1* and *IMP5*, respectively, were selected to follow-up previous work that showed that polymorphism CA3662 is associated with ALS-G and PDC-G (32), because these SNPs had minor allele frequencies in Chamorros $>$5%, and based on LD, provided non-redundant information. SNPs 3–9 in *MAPT* were selected based on work by others on the association between *MAPT* alleles and PSP (35,43,44), and because these SNPs had minor allele frequencies of $>$5% in a panel of 16 Chamorro controls.

Statistical analysis

A χ^2 goodness-of-fit test was used to assess departure from Hardy–Weinberg equilibrium of the genotype frequencies at each SNP in controls and cases. Pairwise LD between SNPs was measured by estimating $|D'|$, the normalized disequilibrium coefficient (72) and the squared correlation coefficient r^2. Fisher's exact test was used to perform global tests to detect allele or genotype frequency differences across three or more groups. Odds ratios (ORs) and 95% CIs were estimated using logistic regression. All analyses were conducted using Stata 9.1 (StataCorp LP, College Station, TX, USA).

To identify potentially interesting SNPs, we performed global tests of allele and genotype frequency differences among the four diagnosis groups (controls, ALS-G, PDC-G and GD). Global tests allow multiple groups to be compared using a single statistical test, thereby protecting against inflated false-positive rates due to multiple comparisons. A global significance level of ~10% was used to select SNPs for more detailed comparisons of the controls and each case group separately. Disease-specific models of the combined effects of multiple SNPs were constructed using

the following procedure. First, univariate logistic regression was performed to identify SNP genotypes associated ($P \leq 0.05$) with a particular disease. Pairs of associated SNPs and their interactions were then included in logistic regression models. SNPs involved in a significant interaction or that remained significant in two-locus models were then assessed in higher order models, and were included in the final model for the disease if they retained their significance. Age, gender and *APOE* genotype were assessed as potential confounders using a 10% change in the ORs for any genetic effect as the criterion for retention in the final model.

ALS-G, PDC-G and GD in Guam may represent pleiotropic effects or variable expressivity of a single altered gene as originally hypothesized for ALS-G and PDC-G by Plato *et al.* (18), or a single set of altered genes. The power of our analyses to detect associations with ALS-G alone was limited because DNA was available from only 54 ALS-G cases. Therefore, the best genetic model as determined by analyses of PDC-G and GD was also fit using only ALS-G cases, as well as all three disease groups combined, compared to the control group.

Haplotype frequencies were estimated with an EM algorithm by the program HAPFREQS (73) in individuals homozygous for the H1 inversion polymorphism. Frequencies were estimated separately in the controls, in each case sample, and in the combined sample, as well as, for comparison, in the HapMap Japanese (JPT) sample as the closest match to Guam in ethnic origin. Haplotype frequencies in the Guam samples were estimated for SNPs 6 and 9, and also for SNPs 4, 6 and 9. The latter 3-SNP haplotypes were used as a surrogate for the three SNPs previously reported to tag the H1c haplotype associated with PSP and CBD (36): rs1467967 (7.2 kb proximal to SNP4), rs242557 (SNP6) and rs2471738 (8.7 kb distal to SNP9). To compare haplotype status of the high-risk haplotype found in the current study with the H1c haplotype, haplotype frequencies were estimated in the JPT sample for all five SNPs. From these frequencies, we computed the conditional probability of haplotype H1c (AxAxT) as P(AxAxT | xTACx) and P(AxAxT | xxACx), where x indicates any SNP allele in a particular haplotype position, A, T,G and C are the particular SNP alleles, and the SNPs are indicated in their chromosomal order: rs1467967–SNP4–SNP6–SNP9–rs2471738. Similar analysis using the Caucasian (CEU) HapMap sample lead to the same conclusion regarding the conditional probability of the H1c haplotype (data not shown).

SUPPLEMENTARY MATERIAL

Supplementary Material is available at HMG Online.

ACKNOWLEDGEMENTS

This work was supported by NIA grant PO1 AG14382, P50 AG 05136, and by the Department of Veterans Affairs. The authors are grateful for the efforts of research assistants and clinicians who have contributed to identifying and evaluating patients in Guam over the years.

Conflict of Interest statement. None of the authors have any conflict of interest.

REFERENCES

1. Kurland, L.T. and Mulder, D.W. (1954) Epidemiologic investigations of amyotrophic lateral sclerosis. 1. Preliminary report on the geographic distribution, with special reference to the Mariana Islands, including clinical and pathologic observations. *Neurology*, **4**, 355–378.
2. Rodgers-Johnson, P., Garruto, R.M., Yanagihara, R., Chen, K.-M., Gajdusek, D.C. and Gibbs, C.J. (1986) Amyotrophic lateral sclerosis and parkinsonism-dementia complex on Guam: a 30-year evaluation of clinical and neuropathologic trends. *Neurology*, **36**, 7–13.
3. Hirano, A., Arumugasamy, N. and Zimmerman, H.M. (1967) Amyotrophic lateral sclerosis. A comparison of Guam and classical cases. *Arch. Neurol.*, **16**, 357–363.
4. Hirano, A., Malamud, N., Elizan, T.S. and Kurland, L.T. (1966) Amyotrophic lateral sclerosis and Parkinsonism-dementia complex on Guam. Further pathologic studies. *Arch. Neurol.*, **15**, 35–51.
5. Hof, P.R., Nimchinsky, E.A., Buee-Scherrer, V., Buee, L., Nasrallah, J., Hottinger, A.F., Purohit, D.P., Loerzel, A.J., Steele, J.C., Delacourte, A. *et al.* (1994) Amyotrophic lateral sclerosis/parkinsonism-dementia complex of Guam: quantitative neuropathology, immunohistochemical analysis of neuronal vulnerability, and comparison with related neurodegenerative disorders. *Acta. Neuropathol.*, **88**, 397–404.
6. Malamud, N., Hirano, A. and Kurland, L.T. (1961) Pathoanatomic changes in amyotrophic lateral sclerosis on Guam. *Neurology*, **5**, 401–414.
7. Hirano, A., Kurland, L.I.T., Krooth, R.S. and Lessell, S. (1961) Parkinson-dementia complex, an endemic disease on the island of Guam. I. Clinical features. *Brain*, **84**, 642–661.
8. Hof, P.R. and Perl, D.P. (2002) Neurofibrillary tangles in the primary motor cortex in Guamanian amyotrophic lateral sclerosis/parkinsonism-dementia complex. *Neurosci. Lett.*, **328**, 294–298.
9. Hirano, A., Malamud, N. and Kurland, L.I.T. (1961) Parkinson-dementia complex, an endemic disease on the island of Guam. II. Pathological features. *Brain*, **84**, 662–679.
10. Matsumoto, S., Hirano, A. and Goto, S. (1990) Spinal cord neurofibrillary tangles of Guamanian amyotrophic lateral sclerosis and parkinsonism-dementia complex: an immunohistochemical study. *Neurology*, **40**, 975–979.
11. Kato, S., Hirano, A., Llena, J.F., Ito, H. and Yen, S.H. (1992) Ultrastructural identification of neurofibrillary tangles in the spinal cords in Guamanian amyotrophic lateral sclerosis and parkinsonism-dementia complex on Guam. *Acta. Neuropathol.*, **83**, 277–282.
12. Galasko, D., Salmon, D., Craig, U.K., Perl, D.P. and Schellenberg, G. (2002) Clinical features and changing patterns of neurodegenerative disorders on Guam, 1997–2000. *Neurology*, **59**, 1121.
13. Galasko, D., Salmon, D.P., Olichney, J. *et al.* (2003) Diverse types of pathology underlie dementia in older Chamorros on Guam. *Neurology*, **60** (Suppl. 1), A329–A330.
14. Koerner, D.R. (1952) Amyotrophic lateral sclerosis on Guam: A clinical study and review of the literature. *Ann. Int. Med.*, **37**, 1204–1220.
15. Kurland, L.T. and Mulder, D.W. (1955) Epidemiologic investigations of amyotrophic lateral sclerosis. 2. Familial aggregations indicative of dominant inheritance. Part II. *Neurology*, **5**, 249–268.
16. Kurland, L.T. and Mulder, D.W. (1955) Epidemiologic investigations of amyotrophic lateral sclerosis. 2. Familial aggregations indicative of dominant inheritance. Part I. *Neurology*, **5**, 182–196.
17. Kurland, L.T. and Mulder, D.W. (1955) Epidemiologic investigations of amyotrophic lateral sclerosis. *Neurology*, **4**, 438–448.
18. Plato, C.C., Cruz, M.T. and Kurland, L.T. (1969) Amyotrophic lateral sclerosis/Parkinsonism dementia complex of Guam: further genetic investigations. *Am. J. Hum. Genet.*, **21**, 133–141.
19. Bailey-Wilson, J.E., Plato, C.C., Elston, R.C. and Garruto, R.M. (1993) Potential role of an additive genetic component in the cause of amyotrophic lateral sclerosis and Parkinsonism-dementia in the Western Pacific. *Am. J. Med. Genet.*, **45**, 68–76.
20. Plato, C.C., Galasko, D., Garruto, R.M., Plato, M., Gamst, A., Craig, U.K., Torres, J.M. and Wiederholt, W. (2002) ALS and PDC of Guam—forty-year follow-up. *Neurology*, **58**, 765–773.
21. Itoh, N., Ishiguro, K., Arai, H., Kokubo, Y., Sasaki, R., Narita, Y. and Kuzuhara, S. (2003) Biochemical and ultrastructural study of neurofibrillary tangles in amyotrophic lateral sclerosis/parkinsonism-dementia complex in the Kii peninsula of Japan. *J. Neuropath. Exp. Neurol.*, **62**, 791–798.

22. Kokubo, Y. and Kuzuhara, S. (2004) Neurofibrillary tangles in ALS and parkinsonism-dementia complex focus in Kii, Japan. *Neurology*, **63**, 2399–2401.
23. Kokubo, Y., Kuzuhara, S. and Narita, Y. (2000) Geographic distribution of amyotrophic lateral sclerosis with neurofibrillary tangles in the Kii peninsula of Japan. *J. Neurol.*, **415**, 850–852.
24. Kuzuhara, S., Kokubo, Y., Sasaki, R., Narita, Y., Yabana, T., Hasegawa, M. and Iwatsubo, T. (2001) Familial amyotrophic lateral sclerosis and parkinsonism-dementia complex of the Kii peninsula of Japan: clinical and neuropathological study and tau analysis. *Ann. Neurol.*, **49**, 501–511.
25. Yase, Y. (1970) Neurologic disease in the western Pacific islands, with a report on the foci of amyotrophic lateral sclerosis found in the Kii peninsula, Japan. *Am. J. Trop. Med. Hyg.*, **19**, 155–166.
26. Garruto, R.M., Yanagihara, R. and Gajdusek, D.C. (1985) Disappearance of high-incidence amyotrophic lateral sclerosis and parkinsonism-dementia on Guam. *Neurology*, **35**, 193–198.
27. Spencer, P.S., Nunn, P.B., Hugon, J., Ludolph, A.C., Ross, S.M., Roy, D.N. and Robertson, R.C. (1987) Guam amyotrophic lateral sclerosis-parkinsonism-dementia linked to plan excitant Neurotoxin. *Science*, **237**, 517–522.
28. Poorkaj, P., Bird, T.D., Wijsman, E., Nemens, E., Garruto, R.M., Anderson, L., Andreadis, A., Wiederholt, W.C., Raskind, M. and Schellenberg, G.D. (1998) Tau is a candidate gene for chromosome 17 frontotemporal dementia. *Ann. Neurol.*, **43**, 815–825.
29. Spillantini, M.G., Murrell, J.R., Goedert, M., Farlow, M.R., Klug, A. and Ghetti, B. (1998) Mutation in the tau gene in familial multiple system tauopathy with presenile dementia. *Proc. Natl. Acad. Sci. U.S.A.*, **95**, 7737–7741.
30. Hutton, M., Lendon, C.L., Rizzu, P., Baker, M., Froelich, S., Houlden, H., Pickering-Brown, S., Chakraverty, S., Isaacs, A., Grover, A. *et al.* (1998) Association of missense and 5′-splice-site mutations in tau with the inherited dementia FTDP-17. *Nature*, **393**, 702–705.
31. Perez-Tur, J., Buee, L., Morris, H.R., Waring, S.C., Onstead, L., Wavrant-De Vrieze, F., Crook, R., Buee-Scherrer, V., Hof, P.R., Petersen, R.C. *et al.* (1999) Neurodegenerative diseases of Guam: analysis of Tau. *Neurology*, **53**, 411–413.
32. Poorkaj, P., Tsuang, D., Wijsman, E.M., Nemens, E., Garruto, R.M., Craig, U., Anderson, L.-J., Bird, T.D., Plato, C.C., Weiderholt, W. *et al.* (2001) Tau is a susceptibility gene for amyotropic lateral sclerosis-parkinsonism dementia complex of Guam. *Arch. Neurol.*, **58**, 1871–1878.
33. Morris, H.R., Steele, J.C., Crook, R., Wavrant-De Vrieze, F., OnsteadCardinale, L., GwinnHardy, K., Wood, N.W., Farrer, M., Lees, A.J., McGeer, P.L. *et al.* (2004) Genome-wide analysis of the Parkinsonism-dementia complex of Guam. *Arch. Neurol.*, **61**, 1889–1897.
34. Conrad, C., Andreadis, A., Trojanowski, J., Dickson, D., Kang, D., Chen, X., Wiederholt, W., Hansen, L., Masliah, E., Thal, L. *et al.* (1997) Genetic evidence for the involvement of Tau in progressive supranuclear palsy. *Ann. Neurol.*, **41**, 277–281.
35. Pastor, P., Ezquerra, M., Perez, J.C., Chakraverty, S., Norton, J., Racette, B.A., McKeel, D., Perlmutter, J.S., Tolosa, E. and Goate, A.M. (2004) Novel haplotypes in 17q21 are associated with progressive supranuclear palsy. *Ann. Neurol.*, **56**, 249–258.
36. Pittman, A.M., Myers, A.J., Duckworth, J., Bryden, L., Hanson, M., Abou-Sleiman, P., Wood, N.W., Hardy, J., Lees, A. and de Silva, R. (2004) The structure of the tau haplotype in controls and in progressive supranuclear palsy. *Hum. Mol. Genet.*, **13**, 1267–1274.
37. Hughes, A., Mann, D. and Pickering-Brown, S. (2003) Tau haplotype frequency in frontotemporal lobar degeneration and amyotrophic lateral sclerosis. *Exp. Neurol.*, **181**, 12–16.
38. Baker, M., Litvan, I., Houlden, H., Adamson, J., Dickson, D., Perez-Tur, J., Hardy, J., Lynch, T., Bigio, E. and Hutton, M. (1999) Association of an extended haplotype in the tau gene with progressive supranuclear palsy. *Hum. Mol. Genet.*, **8**, 711–715.
39. Higgins, J.J., Golbe, L.I., Debiase, A., Jankovic, J., Factor, S.A. and Adler, R.L. (2000) An extended 5′-tau susceptibility haplotype in progressive supranuclear palsy. *Neurology*, **55**, 1364–1367.
40. Di Maria, E., Tabaton, M., Vigo, T., Abbruzzese, G., Bellone, E., Donati, C., Frasson, E., Marchese, R., Montagna, P., Munoz, D.G. *et al.* (2000) Corticobasal degeneration shares a common genetic background with progressive supranuclear palsy. *Ann. Neurol.*, **47**, 374–377.
41. Houlden, H., Baker, M., Morris, H.R., MacDonald, N., Pickering-Brown, S., Adamson, J., Lees, A.J., Rossor, M.N., Quinn, N.P., Kertesz, A. *et al.* (2001) Corticobasal degeneration and progressive supranuclear palsy share a common tau haplotype. *Neurology*, **56**, 1702–1706.
42. Myers, A.J., Kaleem, M., Marlowe, L., Pittman, A.M., Lees, A.J., Fung, H.C., Duckworth, J., Leung, D., Gibson, A., Morris, C.M. *et al.* (2005) The H1c haplotype at the MAPT locus is associated with Alzheimer's disease. *Hum. Mol. Genet.*, **14**, 2399–2404.
43. Rademakers, R., Melquist, S., Cruts, M., Theuns, J., Del-Favero, J., Poorkaj, P., Baker, M., Sleegers, K., Crook, R., De Pooter, T. *et al.* (2005) High-density SNP haplotyping suggests altered regulation of tau gene expression in progressive supranuclear palsy. *Hum. Mol. Genet.*, **14**, 3281–3292.
44. Pittman, A.M., Myers, A.J., Abou-Sleiman, P., Fung, H.C., Kaleem, M., Marlowe, L., Duckworth, J., Leung, D., Williams, D., Kilford, L. *et al.* (2005) Linkage disequilibrium fine mapping and haplotype association analysis of the tau gene in progressive supranuclear palsy and corticobasal degeneration. *J. Med. Genet.*, **42**, 837–846.
45. Stefansson, H., Helgason, A., Thorleifsson, G., Steinthorsdottir, V., Masson, G., Barnard, J., Baker, A., Jonasdottir, A., Ingason, A., Gudnadottir, V.G. *et al.* (2005) A common inversion under selection in Europeans. *Nat. Genet.*, **37**, 129–137.
46. Skipper, L., Wilkes, K., Toft, M., Baker, M., Lincoln, S., Hulihan, M., Ross, O.A., Hutton, M., Aasly, J. and Farrer, M. (2004) Linkage disequilibrium and association of MAPT H1 in Parkinson disease. *Am. J. Hum. Genet.*, **75**, 669–677.
47. Schaid, D.J. and Jacobsen, S.J. (1999) Biased tests of association: comparisons of allele frequencies when departing from Hardy–Weinberg proportions. *Am. J. Epidemiol.*, **149**, 706–711.
48. Poorkaj, P., Kas, A., D'Souza, I., Zhou, Y., Pham, O., Olson, M.V. and Schellenberg, G.D. (2001) A genomic sequence analysis of the mouse and human microtubule-associated protein tau. *Mamm. Genome*, **12**, 700–712.
49. Andreadis, A. (2005) Tau gene alternative splicing: expression patterns, regulation and modulation of function in normal brain and neurodegenerative diseases. *Biochim. Biophys. Acta.*, **1739**, 91–103.
50. D'Souza, I., Poorkaj, P., Hong, M., Nochlin, D., Lee, V.M.Y., Bird, T.D. and Schellenberg, G.D. (1999) Missense and silent tau gene mutations cause front temporal dementia with parkinsonism - chromosome 17 type by affecting multiple alternative RNA splicing regulatory elements. *Proc. Natl Acad. Sci. USA*, **96**, 5598–5603.
51. Friedmann, E., Lemberg, M.K., Weihofen, A., Dev, K.K., Dengler, U., Rovelli, G. and Martoglio, B. (2004) Consensus analysis of signal peptide peptidase and homologous human aspartic proteases reveals opposite topology of catalytic domains compared with presenilins. *J. Biol. Chem.*, **279**, 50790–50798.
52. Cox, P.A. and Sacks, O.W. (2002) Cycad neurotoxins, consumption of flying foxes, and ALS-PDC disease in Guam. *Neurology*, **58**, 956–959.
53. Duncan, M.W., Steele, J.C., Kopin, I.J. and Markey, S.P. (1990) 2-amino-3-(methylamino)-propanoic acid (BMAA) in cycad flour: an unlikely cause of amyotrophic lateral sclerosis and parkinsonism-dementia of Guam. *Neurology*, **40**, 767–772.
54. Garruto, R.M., Yanagihara, R. and Gajdusek, D.C. (1988) Cycads and amyotrophic lateral sclerosis/parkinsonism dementia. *Lancet*, **ii**, 1079.
55. Duncan, M., Kopin, I.J., Garruto, R.M., Lavine, L. and Markey, S.P. (1988) 2-Amino-3 (methylamino)-propionic acid in cycad-derived foods is an unlikely cause of amyotrophic lateral sclerosis/parkinsonism. *Lancet*, **ii**, 631–632.
56. Farrer, L.A., Cupples, L.A., Haines, J.L., Hyman, B., Kukull, W.A., Mayeux, R., Myers, R.H., Pericak-Vance, M.A., Risch, N. and Van Duijn, C.M. (1997) Effects of age, sex, and ethnicity on the association between apolipoprotein E genotype and Alzheimer disease: a meta-analysis. *JAMA*, **278**, 1349–1356.
57. Clark, L.N., Levy, G., Tang, M.X., Mejia-Santana, H., Ciappa, A., Tycko, B., Cote, L.J., Louis, E.D., Mayeux, R. and Marder, K. (2003) The Saitohin 'Q7R' polymorphism and tau haplotype in multi-ethnic Alzheimer disease and Parkinson's disease cohorts. *Neurosci. Lett.*, **347**, 17–20.
58. Russ, C., Powell, J.F., Zhao, J.H., Baker, M., Hutton, M., Crawford, F., Mullan, M., Roks, G., Cruts, M. and Lovestone, S. (2001) The microtubule associated protein Tau gene and Alzheimer's disease - an association study and meta-analysis. *Neurosci. Lett.*, **314**, 92–96.
59. Green, E.K., Thaker, U., McDonagh, A.M., Iwatsubo, T., Lambert, J.C., Chartier Harlin, M.C., Harris, J.M., Pickering-Brown, S.M., Lendon, C.L. and Mann, D.M.A. (2002) A polymorphism within intron 11 of the tau gene is not increased in frequency in patients with sporadic Alzheimer's

disease, nor does it influence the extent of tau pathology in the brain. *Neurosci. Lett.*, **324**, 113–116.
60. Streffer, J.R., Papassotiropoulos, A., Kurosinski, P., Signorell, A., Wollmer, M.A., Tsolaki, M., Iakovidou, V., Horndli, F., Bosset, J., Gotz, J. *et al.* (2003) Saitohin gene is not associated with Alzheimer's disease. *J. Neurol. Neurosurg. Psychiatry*, **74**, 362–363.
61. Verpillat, P., Richard, S., Hannequin, D., Dubois, B., Bou, J., Camuzat, A., Pradier, L., Frebourg, T., Brice, A., Clerget-Darpoux, F. *et al.* (2002) Is the saitohin gene involved in neurodegenerative diseases? *Ann. Neurol.*, **52**, 829–832.
62. Oliveira, S.A., Martin, E.R., Scott, W.K., Nicodemus, K.K., Small, G.W., Schmechel, D.E., Doraiswamy, P.M., Roses, A.D., Saunders, A.M., Gilbert, J.R. *et al.* (2003) The Q7R Saitohin gene polymorphism is not associated with Alzheimer disease. *Neurosci. Lett.*, **347**, 143–146.
63. Cook, L., Brayne, C.E., Easton, D., Evans, J.G., Xuereb, J., Cairns, N.J. and Rubinsztein, D.C. (2002) No evidence for an association between Saitohin Q7R polymorphism and Alzheimer's disease. *Ann. Neurol.*, **52**, 690–691.
64. Kwon, J.M., Nowotny, P., Shah, P.K., Chakraverty, S., Norton, J., Morris, J.C. and Goate, A.M. (2000) Tau polymorphisms are not associated with Alzheimer's disease. *Neurosci. Lett.*, **284**, 77–80.
65. Tanahashi, H., Asada, T. and Tabira, T. (2004) Association between tau polymorphism and male early-onset Alzheimer's disease. *Neuroreport*, **15**, 175–179.
66. Combarros, O., Rodero, L., Infante, J., Palacio, E., Llorca, J., Fernandez-Viadero, C., Pena, N. and Berciano, J. (2003) Age-dependent association between the Q7R polymorphism in the saitohin gene and sporadic Alzheimer's disease. *Dement. Geriat. Cog. Disord.*, **16**, 132–135.
67. Conrad, C., Vianna, C., Freeman, M. and Davies, P. (2002) A polymorphic gene nested within an intron of the tau gene: implications for Alzheimer's disease. *Proc. Natl Acad. Sci. USA*, **99**, 7751–7756.
68. Bullido, M.J., Aldudo, J., Frank, A., Coria, F., Avila, J. and Valdivieso, F. (2000) A polymorphism in the tau gene associated with risk for Alzheimer's disease. *Neurosci. Lett.*, **278**, 49–52.
69. Peplonska, B., Zekanowski, C., Religa, D., Czyzewski, K., Styczynska, M., Pfeffer, A., Gabryelewicz, T., Golebiowski, M., Luczywek, E., Wasiak, B. *et al.* (2003) Strong association between Saitohin gene polymorphism and tau haplotype in the Polish population. *Neurosci. Lett.*, **348**, 163–166.
70. McKhann, G., Drachman, D., Folstein, M., Katzman, R., Price, D. and Stadlan, E.M. (1984) Clinical diagnosis of Alzheimer's disease: report on the NINCDS-ADRDA work group under the auspices of the Department of Human Services Task Force on Alzheimer's disease. *Neurology*, **34**, 939–944.
71. Hixson, J.E. and Vernier, D.T. (1990) Restriction isotyping of human apolipoprotien E by gene amplification and cleavage with Hhal. *J. Lipid Res.*, **31**, 545–548.
72. Lewontin, R.C. (1988) On measures of gametic disequilibrium. *Genetics*, **120**, 849–852.
73. Goddard, K.A.B., Yu, C.E., Oshima, J., Miki, T., Nakura, J., Piussan, C., Martin, G.M., Schellenberg, G.D., Wijsman, E.M., Brown, W.T. *et al.* (1996) Toward localization of the Werner syndrome gene by linkage disequilibrium and ancestral haplotyping: lessons learned from analysis of 35 chromosome 8p11.1-21.1 markers. *Am. J. Hum. Genet.*, **58**, 1286–1302.

Temporal Profiles of Axon Terminals, Synapses and Spines in the Ischemic Penumbra of the Cerebral Cortex

Ultrastructure of Neuronal Remodeling

Umeo Ito, MD, PhD, FAHA; Toshihiko Kuroiwa, MD, PhD; Jun Nagasao, DVM; Emiko Kawakami, BS; Kiyomitsu Oyanagi, MD, PhD

Background and Purpose—Because the recovery process of axon terminals, synapses, and spine-dendrites in the ischemic penumbra of the cerebral cortex is obscure, we studied the temporal profile of these structures up to 12 weeks after the ischemic insult, using a gerbil model.

Methods—Stroke-positive animals were selected according to their stroke index score during the first 10-minute left carotid occlusion done twice with 5-hour interval. The animals were euthanized at various times after the second ischemic insult. Ultra-thin sections including the 2nd to 4th cortical layers were obtained from the neocortex coronally sectioned at the infundibular level, in which the penumbra appeared. We counted the number of synapses, spines and multiple synapse boutons, measured neurite thickness, and determined the percent volume of the axon terminals and spines by Weibel point counting method.

Results—The number of synapses, synaptic vesicles and spines and the total percent volume of the axon terminals and spines decreased until the 4th day. From 1 to 12 weeks after the ischemic insult, these values increased to or exceeded the control ones, and neuritic thickening and increase in number of multiple synapse boutons occurred.

Conclusions—In the ischemic penumbra, the above structures degenerated, with a reduction in their number and size, until 4 days and then recovered from 1 to 12 weeks after the ischemic insult. (***Stroke*. 2006;37:2134-2139.)**

Key Words: axon terminal ■ dendrites ■ spine ■ synapses ■ transient cerebral ischemia

Cerebral infarction develops rapidly after a large ischemic insult. Earlier we developed a model of temporary ischemia in which a focal infarction surrounded by a large penumbra was produced in the cerebral cortex of Mongolian gerbils by giving a threshold amount of ischemic insult to induce focal infarction.[1,2]

Concerning the neuronal recovery, recent findings have revealed that synapses and their networks express a high degree of functional and structural plasticity.[3] Ultrastructural changes in the postsynaptic density in hippocampal CA-1 were investigated after temporary ischemia.[4–6] Degenerated boutons and multiple synapse boutons (MSBs) in this region were investigated by electron microscopy (EM) after temporary ischemia,[7–9] as well as after temporary hypoxia/hypoglycemia in hippocampal slices.[10] Changes in spines and dendrites were studied by time-lapse microscopy after temporary anoxia/hypoglycemia in cell culture,[11,12] by light microscopy (LMS) of Golgi stain-impregnated sections of the 3rd to 5th cortical layers of the cerebral cortex after temporary ischemia,[13] and by EM after temporary hypoxia/glycemia in hippocampal slice.[10] Changes in CA-1 dendrites after temporary ischemia were investigated by light microscopy of horseradish peroxidase-injected specimens,[14] by EM after temporary ischemia in CA-1,[15,16] and by EM of Golgi stain-impregnated cerebral cortex after temporary ischemia for 20 minutes.[17]

Almost all of the above studies were performed in connection with delayed ischemia-induced injury to CA-1 neurons, and observations were made during a short period after ischemia. However, clinically, most patients show gradual recovery from behavioral dysfunctions after a stroke. The long-term integrated profile of axon terminals, synapses, spines, and dendrites during the recovery stage after an ischemic insult has remained obscure, especially in the ischemic penumbra of the cerebral cortex.

Because no functional recovery is anticipated in the infarction itself,[18–20] we aimed to elucidate neuronal remodeling process in the ischemic penumbra in which neuronal death progresses in a disseminated fashion,[2,18,20] by focusing on the temporal profiles of axon terminals, synapses, spines, and neurites.

Materials and Methods

Under anesthesia with 2% halothane, 70% nitrous oxide, and 30% oxygen, the left carotid artery of adult male Mongolian gerbils (60 to

Received February 15, 2006; final revision received May 1, 2006; accepted May 24, 2006.

From the Department of Neuropathology (U.I., J.N., E.K., K.O.), Tokyo Metropolitan Institute for Neuroscience, Tokyo, Japan; and the Department of Neuropathology (T.K.), Medical Research Institute, Tokyo Medical and Dental University, Tokyo, Japan.

Correspondence to Umeo Ito, MD, PhD, FAHA, Department of Neuropathology, Tokyo Metropolitan Institute for Neuroscience, Tokyo, 2-6, Musashidai, Fuchu-shi, Tokyo 183-8526, Japan. E-mail umeo-ito@nn.iij4u.or.jp

Stroke is available at http://www.strokeaha.org

DOI: 10.1161/01.STR.0000231875.96714.b1

80 g) was twice occluded with a Heifetz aneurismal clip for 10 minutes each time, with a 5-hour interval between the 2 occlusions, anesthesia was discontinued immediately after each cervical surgery, the animals soon became awake and moved spontaneously.

Ischemia-positive animals registering >13 points were selected based on the stroke index score determined during the first occlusion.[21] The gerbils were euthanized at various times, ie, at 5, 12, 24, 48-hour, 4 days, and 1, 5, 8, and 12 weeks after the ischemic insult. Anesthetization was followed by intracardiac perfusion with diluted fixative (1% paraformaldehyde, 1.25% glutaraldehyde in 0.1 mol/L cacodylate buffer) for 5 minutes, followed by perfusion with concentrated fixative (4% paraformaldehyde, 5% glutaraldehyde in 0.1 mol/L cacodylate buffer) for 20 minutes for EM (3 animals in each time group), or with 10% phosphate-buffered formaldehyde fixative for 30 minutes for LMS (5 animals in each time group).

In this model, after the restoration of blood flow, only ischemic penumbra with progressing disseminated selective neuronal necrosis (DSNN) appeared in the coronal face sectioned at the infundibular level (Face B) and focal infarction evolved among the DSNN in the coronal face sectioned at the chiasm (Face A). Ultra-thin sections including the 2nd to 4th cortical layers were prepared from the left cerebral cortex at the mid-point between the interhemispheric and rhinal fissures on Face B, penumbra >1 mm caudal to infarction edge. The sections were double stained with uranyl acetate and lead solution, and observed with an electron microscope (H9000, Hitachi). Paraffin sections of both faces were separately stained with hematoxylin-eosin (HE) or periodic acid fuchsin Schiff (PAS) or by Bodian silver impregnation or used for immunohistochemical detection of glial fibrillary acidic protein.

Placing 1.0 cm×1.0 cm quadratic lattices of points on 5000×2.67 times enlarged EM photographs, we measured the number of synapses (synapses: consist of the pre- and postsynaptic densities associated with their cytoplasmic faces, and the synaptic cleft between them) and spines (spines: an ovoid bulb that is filled with a fluffy material and connected to dendrite directly or by a stalk) in the neuropil in a 100-cm^2 area (56 μm^2, by real size) by examining 1800±364 cm^2 in the neuropil of 3 animals in each time group. We determined the percent volume of the axon terminals (axon terminals: presynaptic expansion of the axon that contains synaptic vesicles and mitochondria) and spines by using the point counting method[22] in which the number of intersecting points touched by the axon terminals and/or spines were counted among 1000 to 15 000 points (counting number varied according to the equation of the relative error for different volumetric proportions) of the quadratic lattice in each time group. We measured the thickness of 194±38 neurites (neurites: axons and dendrites those contain microtubules, neurofilaments and mitochondria; differentiation between them in transverse section is often difficult, especially in small ones) in each time group, as the maximal diameter perpendicular to their neurofilaments and/or microtubules. We also measured the percentage of MSBs by counting 327±38 synapses in each time group, all on the same EM pictures. The statistical differences between each of the time groups were analyzed by ANOVA, followed by Bonferroni-Dunn test. All data in the Table and Figure 6 were presented as average±SEM and a statistical difference was accepted at $P<0.05$ level.

Results

In the ischemic penumbra of the cerebral cortex in Face B, eosinophilic ischemic neurons (HE staining) appeared in disseminated fashion among the normal-looking neurons in the 2nd to 6th cortical layers by LMS, around 5 hours after the ischemic insult. Some of these eosinophilic cell bodies became remarkably shrunken and died during the period of 12 to 48 hours, which indicates DSNN (Figure 1A). The eosinophilic ischemic neurons were found by EM to be disseminated electron-dense dark neurons that increased in number during the period of 12 to 48 hours after the ischemic insult.

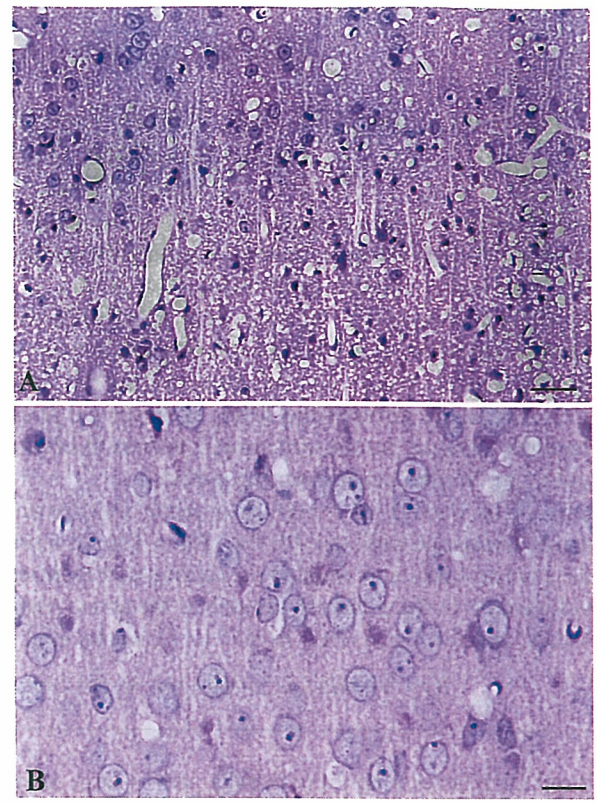

Figure 1. Light-microscopy of 2nd to 4th cortical layers of the cerebral cortex in Face B. A, Twenty-four hours after the ischemic insult, some of the eosinophilic ischemic neurons show marked shrinkage compared with the more normal-looking neurons, indicating disseminated selective neuronal necrosis. These abnormal neurons increased in number until day 2 to 3 postischemia (HE, Bar 31.3 μm). B, Eight weeks after the ischemic insult. The eosinophilic ghost cells of faintly formed cell bodies are reduced in size and are found in the 3rd cortical layer (PAS, Bar 12.5 μm).

From 4 days until 8 weeks, these condensed electron-dense dark neurons became fragmented into an accumulation of electron-dense granular fragments, which were observed by LMS as eosinophilic ghost cells of faintly formed cell bodies by HE and PAS staining (Figure 1B). During 2 to 12 weeks, these eosinophilic ghost cells accumulated in the 3rd and occasionally in the 5th cortical layer decreasing in size because of loss of their periphery (Figure 1B). In Face A, focal infarction evolved and developed among the DSNN from 12 hours to 4 days.

From 4 days to 12 weeks after the ischemic insult, the axon terminals of the surviving neurons were found being attached

Percent of MSBs Among Synapses

	Control	5 Hours	4 Days	1 Week	5 Weeks	8 Weeks	12 Weeks
% MSBs	1.76±0.82	0.85±0.84	0.86±0.67	1.18±0.75	0.45±0.45	3.14±0.85	6.93±2.24*

*Compared with control, 4 days, and 8 weeks; $P<0.05$.

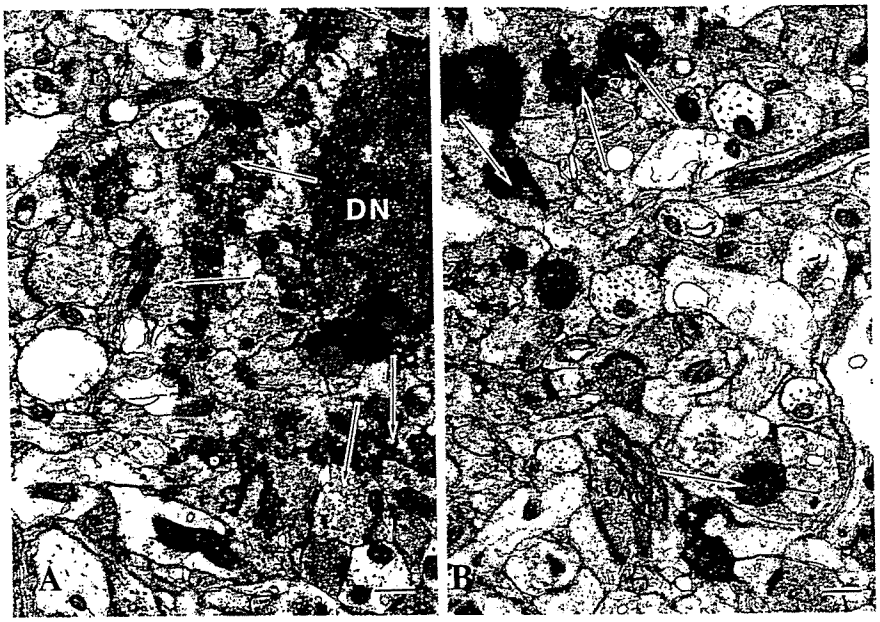

Figure 2. Electron microscopy of 3rd layer of the cerebral cortex in Face B, 1 week after the ischemic insult. A, The axon terminals of the surviving neurons make contact with the periphery of the accumulated fragments of electron-dense granules of dead neurons (DN). Some of them appeared to have pinched off pieces of the dead neurons, and are encrusted by the electron-dense granular fragments of the dead neurons (arrows). Bar 2.3 μm. B, Some axon terminals are found attached to the electron dense thick neurites of dead neurons (arrows). Bar 2.6 μm.

to the peripherally located electron-dense granular fragments and dendritic portions of the shrunken dark neurons. Some of these terminals appeared to have pinched off pieces of the dead neurons, and they bore a crust of the electron-dense granular fragments of the dead neurons (Figure 2A). Other axon terminals were found attached to the electron-dense thick neurites of dead neurons (Figure 2B). Some of the fragment-encrusted axon terminals were occasionally observed to have synapsed with the spines and neurites of the surviving neurons (Figure 3A). Some axons connected to the dying neurons showed globular and abnormal distensions of their terminals as seen by silver impregnation (Figure 4A). These structures appeared as degenerated axon by EM. The amplified degenerated axon contained degenerated mitochondria, laminated dense bodies, and irregularly located neurofilaments and microtubules; the degenerated axon occasionally made synapses onto adjacent structures (inset of Figure 4A).

Such axons were often observed around the accumulations of the fragmented electron-dense granular pieces of the dead neurons (Figure 4B).

By 12 weeks after the ischemic insult, neuritic shafts and their branches were remarkably thickened (Figure 5B) compared with those at day 4 (Figure 5A), and they made synapses with voluminously enlarged and occasionally sprouting polygonal axons terminals filled with synaptic vesicles (Figure 5B). MSBs[23] of the axons terminals (Figure 3B) increased in frequency compared with those of the control animals (Table).

The percent volume of the total axon terminals (Figure 6A) and spines (Figure 6B) in the neuropil decreased drastically to 30.9% and 24.8%, respectively, of the control value at that

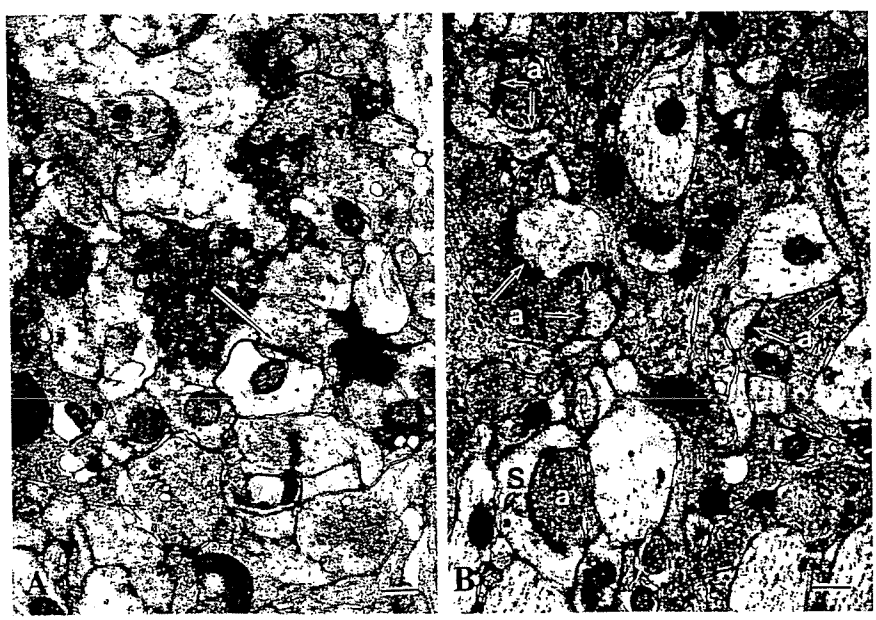

Figure 3. A, Electron microscopy of the 3rd cortical layer in Face B, 1 week after the ischemic insult. Some axon terminals encrusted by the electron-dense granular fragments of the dead neurons are occasionally observed to have made synapses with the spines and neurites of the surviving neurons (arrow). Bar 3.1 μm. B, Electron microscopy of 3rd cortical layer of the cerebral cortex in Face B, 12 weeks after the ischemic insult. MSBs with >2 spines synapsed (arrows) to 1 axon terminal (a). A widened spine(s) with multiple synapses on axon terminal (a) is seen. Bar 3.2 μm.

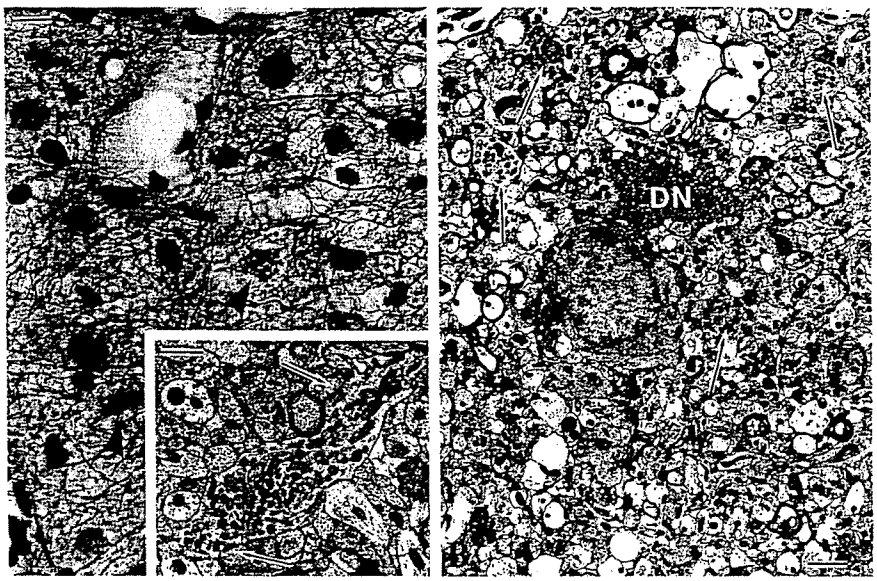

Figure 4. A, Light-microscopy. Four days after the ischemic insult, some axons attached to dying neurons show globular and abnormal distension of their terminals (arrow-heads). Bar 8.9 μm. Bodian's silver impregnation. Inset: EM observation of the distended degenerated axon 3 weeks after the ischemic insult. It contains degenerated mitochondria, laminated dense bodies, and irregularly located neurofilaments and microtubules and has synapses along its wall (arrows). Bar 1.3 μm. B, Electron microscopy of the 3rd layer of the cerebral cortex in Face B, 2 weeks after the ischemic insult. These amplified degenerated axons (arrows) are observed around accumulations of the fragmented electron-dense granular pieces of the dead neurons (DN). Bar 0.6 μm.

time after the ischemic insult, with a decrease in frequency of synaptic vesicles especially those close to the synapses (Figure 5A). The number of synapses also decreased to 73.5% of the control value at 4 days, after a temporary increase up to 135% at 5 hours after the ischemic insult (Figure 6A). The number of spines also decreased to 35.8% of the control value (Figure 6B), by 4 days. From 1 to 12 weeks after the ischemic insult, the percent volume of the total axon terminals (Figure 6A) and the percent volume of the total spines (Figure 6B) increased, being 162.8% and 86.7%, respectively, of the control value at 12 weeks. The number of synapses (Figure 6A) and spines (Figure 6B) also rose, becoming 113.2% and 91.9%, respectively, of it at that time.

The average thickness of neurites in the neuropil of the control animals were 0.607 μm. This value was unchanged at 0.587 μm at day 4, 0.604 μm at 1 week, and 0.665 μm at 8 weeks, and increased to 0.934 μm at 12 weeks after the ischemic insult (Figure 6C).

Discussion

In the neuropils of the ischemic penumbra in the cerebral cortex, we found a marked decrease in the number of the synapses and volume of the axon terminals from 5 hours to 4 days after the ischemic insult, along with a decrease in the number of synaptic vesicles. These changes may be attributed to a demolished synaptic neurotransmission attributable to calcium-dependent neuronal hyperexcitation[4-6] and could be reduced by NMDA (*N*-methyl-D-asparate) receptor antagonists as was reported in a morphological study recording excitatory postsynaptic potential from hippocampal slice cultures subjected to brief anoxia-hypoglycemia.[10]

Almost in accordance with our present study, the LMS study of Golgi silver impregnated spine and dendrites showed that the number of spines and thickness of dendrites decreased maximally in 4 to 7 days after the temporary ischemia and recovered around 5 weeks in the 2nd to 3rd cortical layers of the rat cerebral cortex.[13] Earlier studies on cultured

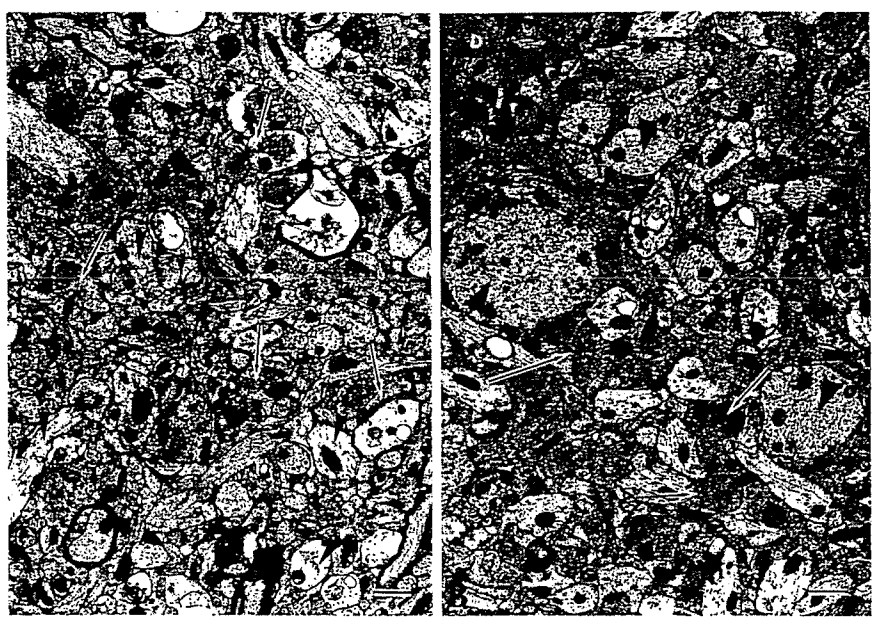

Figure 5. Electron microscopy of the 3rd layer of the cerebral cortex in Face B. A, Four days after the ischemic insult. The volume of axon-terminals and spines has decreased with a decrease in frequency of synaptic vesicles, especially those close to the synapse (arrows). The thickness of degenerated neurites has decreased slightly compared with that of the control (arrowheads). Bar 1.5 μm. B, Twelve weeks after the ischemic insult. The neuritic shafts and their branches are remarkably thickened (arrowheads) and make synapses with voluminously enlarged and occasionally sprouting polygonal axon terminals filled with synaptic vesicles (arrows). Bar 1.5 μm.